PHYSICAL REVIEW B **73**, 165317 (2006)

Photoluminescence investigation of the carrier recombination processes in ZnO quantum dots and nanocrystals

Vladimir A. Fonoberov, Khan A. Alim, and Alexander A. Balandin*
Nano-Device Laboratory, Department of Electrical Engineering, University of California—Riverside, Riverside, California 92521

Faxian Xiu and Jianlin Liu
Quantum Structures Laboratory, Department of Electrical Engineering, University of California—Riverside, Riverside, California 92521

(Received 15 November 2005; revised manuscript received 9 February 2006; published 17 April 2006)

The carrier recombination processes in ZnO quantum dots (~4 nm in diameter), ZnO nanocrystals (~20 nm in diameter) and bulk ZnO crystal have been studied using photoluminescence (PL) spectroscopy in the temperature range from 8.5 to 300 K. The obtained experimental data suggest that the ultraviolet PL in ZnO quantum dots originates from recombination of the acceptor-bound excitons for all temperatures. In the larger size ZnO nanocrystals, the recombination of the acceptor-bound excitons is the dominant contribution to PL only at low temperature ($T < 150$ K). For higher temperatures ($T > 150$ K), PL is mostly due to recombination of the donor-bound excitons. Recombination processes in ZnO quantum dots and nanocrystals differ from those in bulk ZnO mainly because of the large surface-to-volume ratio in both types of nanoparticles and, consequently, a large number of acceptor defects near the surface. No strong inhomogeneous broadening has been observed in ultraviolet PL from ZnO quantum dots. Our results shed light on the carrier-recombination processes in ZnO quantum dots and nanocrystals, and can be used for the ZnO nanostructure optimization for the proposed optoelectronic and spintronic applications.

DOI: 10.1103/PhysRevB.73.165317 PACS number(s): 78.67.Hc, 78.67.Bf, 78.55.−m, 63.22.+m

I. INTRODUCTION

ZnO-based nanostructures have recently attracted attention due to their potential applications in spintronic and ultraviolet (UV) to violet light-emitting and other optoelectronic devices. It is expected that in ZnO nanostructures one may eliminate some unwanted properties of bulk ZnO, such as weak exciton emission in comparison with the defect related (deep-level) visible emission, while keeping or enhancing the desirable properties such as large exciton binding energy (~60 meV). The large exciton binding energy and strong exciton emission would allow for stable high-yield luminescence from ZnO nanostructures even at room temperature. Understanding the carrier recombination processes in ZnO nanostructures and the role of defects is essential not only for the optoelectronic devices but also for the spintronic applications.[1] For example, it was suggested that bound acceptors mediate the ferromagnetic ordering in ZnO.[2] Since doping of semiconductor nanocrystals (NCs) is a rather challenging task,[3] the existence of various unintentional "useful" impurities in ZnO[4] may be advantageous for spintronics and optoelectronics.

The envisioned spintronic and optoelectronic applications of ZnO nanostructures motivated a number of theoretical[5,6] and experimental[7–30] studies of the optical properties of ZnO quantum dots (QDs),[5–14] nanowires,[15] prisms,[16] rods,[17] whiskers,[18] as well as nanocrystalline films[19–21] and thin films.[22–30] Despite many phenomenological studies, the exact mechanisms of UV photoluminescence (PL) and carrier recombination processes in ZnO nanostructures are still subjects of considerable debates. While most of the reports indicate that very-low-temperature (~10 K) UV emission is due to the donor-bound excitons,[17–19,25–27] there is no agreement about the mechanism of the emission at higher temperatures. Various investigations arrived at different and, sometimes, opposite conclusions about the origin of UV PL in ZnO nanostructures. Namely, UV PL was attributed to the confined excitons,[7,8,16,24–26] transverse optical phonon band of the confined excitons,[19,20] donor-bound excitons,[16,18,27] acceptor-bound excitons,[21–23] or donor-acceptor pairs.[15,17,28–30]

Here we report results of the PL investigation of the carrier recombination processes in two types of ZnO nanostructures, i.e., ZnO QDs and ZnO NCs. The distinction between these two nanostructure types is related to their size in comparison with the exciton diameter in ZnO. The average QD diameter is 4 nm, which is of the order of the exciton diameter in ZnO (~2 nm), while the average diameter of ZnO NCs is 20 nm, which is much larger than the exciton diameter. This means that if the QDs were close to ideal (without defects) the charge carriers were in the regime of intermediate quantum confinement.[5] Although the charge carriers do not experience quantum confinement effects in ZnO NCs, their recombination properties are expected to be different from those of bulk ZnO due to the larger surface-to-volume ratio in NCs. Since QDs have even larger surface-to-volume ratio, the presence of many surface defects may affect the emission properties of ZnO QDs stronger than the quantum confinement. The PL spectra obtained for ZnO QDs and NCs have been compared with those obtained for a reference bulk ZnO sample.

II. ROOM TEMPERATURE PL FROM ZnO QDs AND NCs

ZnO QDs and NCs were produced by the wet chemistry method (see the high-resolution transmission electron mi-

 ©2006 The American Physical Society

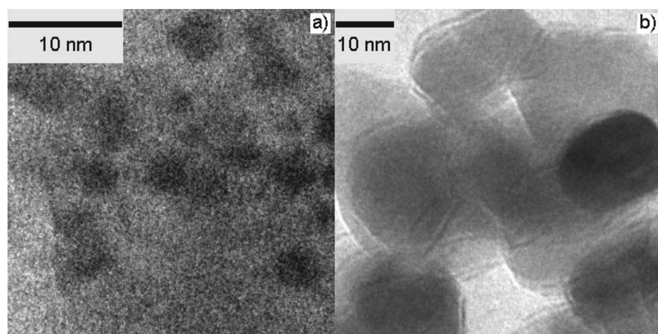

FIG. 1. TEM images of (a) ZnO quantum dots with the average diameter of 4 nm and (b) ZnO nanocrystals with the average diameter of 20 nm.

croscopy (TEM) images in Fig. 1). The examined ZnO QDs and NCs were nearly spherical in shape with the average diameter of 4 and 20 nm, respectively. The size distribution, estimated from the TEM study, was around 20%. As a reference sample we studied a bulk ZnO crystal (University Wafers) with dimensions $5 \times 5 \times 0.5$ mm^3 and *a*-plane $(11\bar{2}0)$ facet. PL spectra of all samples were excited with a He-Cd laser ($\lambda = 325$ nm) and recorded with an Oriel monochromator.

Figure 2 shows typical room temperature PL spectra of ZnO QDs, NCs, and reference bulk sample. Due to the intrinsic defects, which are always present in ZnO,[4] PL spectra of ZnO nanostructures and bulk crystals exhibit deep-level visible emission in addition to the near band-edge UV emission. It is seen from Fig. 2 that the intensity of the UV peak increases with decreasing the nanoparticle size, i.e., as one goes from the bulk ZnO to NCs and to QDs. The highest UV PL yield is observed for ZnO QDs. Visible region of PL for all samples consists of the strong green and rather weak red emission bands. With the decrease of the nanoparticle size, the green deep-level peak moves slightly into the cyan region. For ZnO QDs, the shift of this peak toward higher energy is about 120 meV with respect to its position in the bulk. It is important to note that the intensity of the visible PL bands does not increase with the decrease of the nanoparticle size.

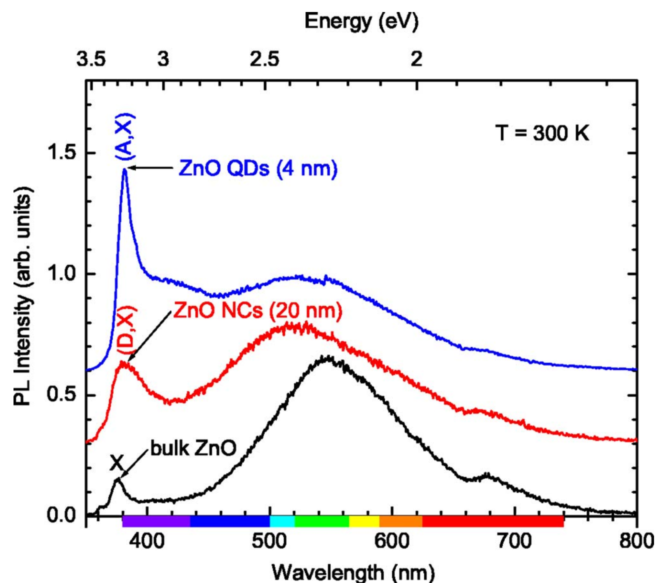

FIG. 2. (Color online). Room temperature PL spectra of 4 nm ZnO quantum dots, 20 nm ZnO nanocrystals, and bulk ZnO (*a* plane). The spectra are shifted in the vertical direction for clarity. For ZnO quantum dots, UV emission at 3.250 eV is attributed to the acceptor-bound excitons. For ZnO nanocrystals, UV emission at 3.250 eV is attributed to the donor-bound excitons. For bulk ZnO, UV emission at 3.294 eV is attributed to the free excitons. Visible emission is defect-related for all samples. The spectra are uncorrected for the grating response.

One can also see from Fig. 2 that the linewidth of the UV emission peak from ZnO QDs is almost the same as that from bulk ZnO. The full width at half maximum (FWHM) is 95, 172, and 86 meV for the ZnO QDs, NCs, and bulk, respectively. The quantum confinement of free excitons in QDs is expected to result in the blueshift of the emission peak, while the size distribution should lead to inhomogeneous broadening of the exciton peaks. Figure 2 shows no additional inhomogeneous broadening and a very small redshift of the UV peak. While in bulk ZnO the UV PL peak is observed at 3.294 eV, PL peaks in UV emission from ZnO QDs and NCs are observed at the same energy of 3.250 eV. As a possible explanation, one can assume that UV PL from ZnO QDs and NCs originates from the recombination of bound excitons. The 44 meV energy difference between the bound exciton peak in ZnO QDs and the free exciton peak in bulk ZnO extracted from our measurements is very close to the reported value of acceptor-exciton localization energy in bulk ZnO of about 50 meV.[21–23,25] Unlike in the case of free excitons, the quantum confinement of acceptor-bound excitons in ZnO QDs is not expected to result in a substantial blueshift of acceptor-bound exciton emission peaks because acceptors are relatively deep impurities for ZnO.[5,28–30] At the same time, donors are rather shallow impurities in ZnO and the donor-bound emission peaks could be strongly affected by quantum confinement.

III. LOW-TEMPERATURE PL FROM ZnO QDs AND NCs

In order to verify that the recombination of the impurity-bound excitons is responsible for the observed PL features, we conducted the low-temperature PL measurements for ZnO QDs, NCs, and bulk samples. Figure 3(a) shows the UV region of the PL spectrum from bulk ZnO for temperatures from 8.5 to 150 K. According to their energy values, the emission peaks (going from right to left) have been assigned to free excitons (X), donor-bound excitons (D, X), acceptor-bound excitons (A, X), and two longitudinal optical (LO) phonon peaks of the donor-bound excitons. One can see that at low temperature, the emission from the free and donor-bound excitons represents two competing carrier recombination processes. In Figs. 3(b) and 3(c), we present the PL peak energies and PL peak intensities for the emission from the free and donor-bound excitons extracted from Fig. 3(a). Depending on the temperature, the donor-exciton localization energy is 10–15 meV, while the acceptor-exciton localization energy is 45–55 meV. As seen from Figs. 3(a) and 3(b),

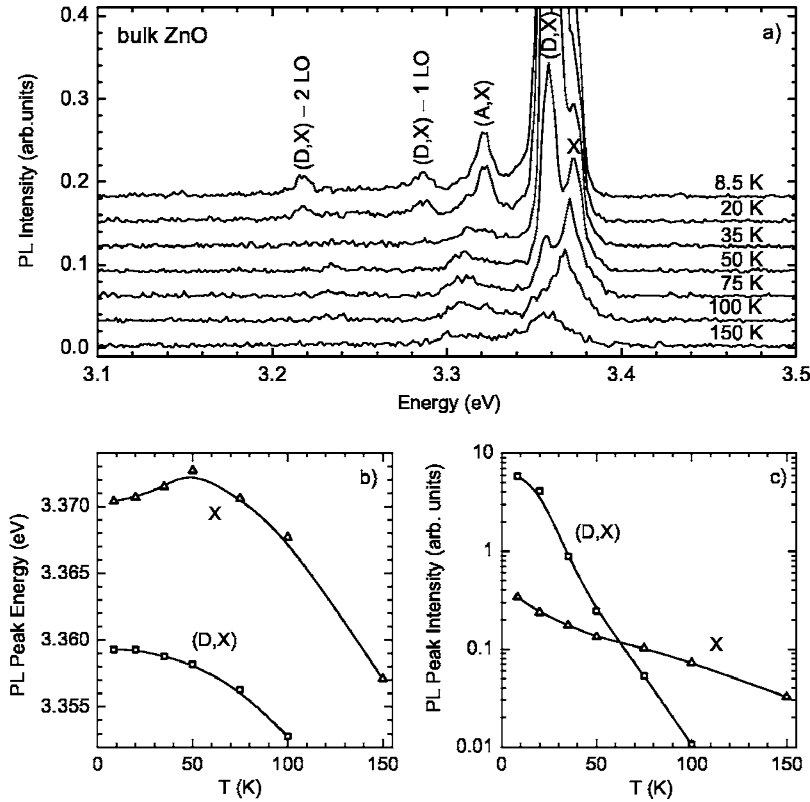

FIG. 3. (a) PL spectra of bulk ZnO (*a* plane) at temperatures from 8.5 to 150 K. The spectra are shifted in the vertical direction for clarity. (b) Peak energies for the free and donor-bound excitons as a function of temperature. (c) Log plot of the free and donor-bound exciton peak intensities as a function of temperature.

the free exciton, donor-bound exciton, and acceptor-bound exciton energies decrease with temperature according to the Varshni law[31]

$$E(T) = E(0) - \frac{\alpha T^2}{T + \theta_D}, \quad (1)$$

where $E(0)$ is the energy at temperature $T=0$ K, α is a parameter, and θ_D is the Debye temperature. The energies $E(0)$ and parameters α calculated for the observed peaks are very close to those reported for ZnO thin films[25] and bulk ZnO[32] (a direct comparison is not possible since different studies employed very different values of θ_D). Table I summarizes parameters of Eq. (1) extracted from our measurements for the above recombination processes (we assumed $\theta_D=920$ K according to Ref. 33).

Figure 3(c) shows that the donor-bound emission dominates in the PL spectra for temperatures below 60 K. For temperatures above 60 K, the free exciton recombination is the main mechanism of PL in bulk ZnO. This temperature is close to the ionization temperature for many types of donor impurities in semiconductors. It is also interesting to note that one- and two-phonon bands are observed for the donor-bound exciton at the lowest temperatures, while no phonon bands are observed for free excitons at higher temperatures. The observed phonon energy 71 meV ($574\ \mathrm{cm}^{-1}$) corresponds to A_1(LO) phonons in ZnO.[13,14]

TABLE I. Parameters of Varshni law for the free and bound excitons in bulk ZnO and ZnO quantum dots ($\theta_D=920$ K).

	$E(0)$ [eV]	α [meV/K]
Bulk ZnO:		
X	3.377	1.10
(D, X)	3.360	0.67
ZnO QDs:		
(D, X)	3.365	1.14
(A, X)	3.313	0.83

Analysis of the low-temperature PL from ZnO QDs and NCs and its comparison with PL from bulk ZnO allows one to determine the main features of the carrier recombination in ZnO nanostructures near the band edge. Figure 4(a) shows UV region of PL spectrum of ZnO NCs for temperatures from 8.5 to 150 K. Assuming that the energy of free excitons in 20 nm ZnO NCs should be almost the same as in bulk ZnO and using the same order of peaks as in the case of PL from bulk ZnO, the broad peak observed at about 3.20 eV can be assigned to the acceptor-bound excitons (A, X) and the peak (shoulder) observed at about 3.35 eV can be assigned to the donor-bound excitons (D, X). Figures 4(b) and 4(c) show the PL peak energies and the PL peak intensities of the donor-bound and acceptor-bound excitons extracted from Fig. 4(a). The dashed curve in Fig. 4(b) shows, as a reference, the free exciton energy from Fig. 3(b). As expected, one can see from Fig. 4(b) that the donor-bound exciton energy in 20 nm ZnO NCs is very close to the bulk value. At the same time, a comparison of the acceptor-bound exciton energies in 20 nm ZnO NCs and in bulk ZnO shows a decrease of about 120 meV for ZnO NCs. The observed significant decrease of the acceptor-bound exciton energy is most likely due to a different kind of acceptors in ZnO NCs. For example, zinc vacancies in ZnO NCs form acceptor lev-

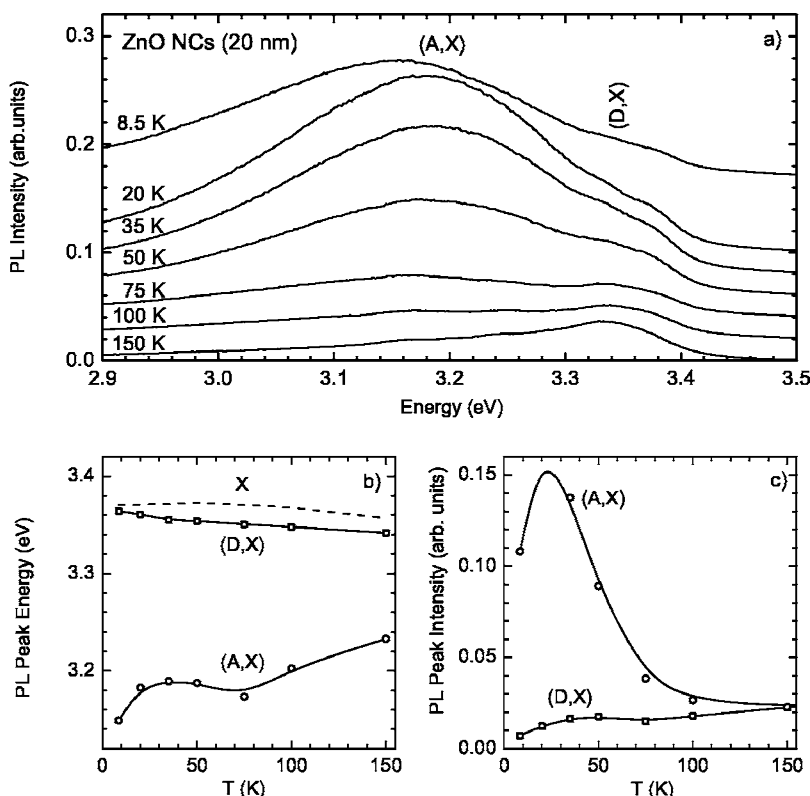

FIG. 4. (a) PL spectra of ZnO nanocrystals (20 nm) at temperatures from 8.5 to 150 K. The spectra are shifted in the vertical direction for clarity. (b) Peak energies for the donor- and acceptor-bound excitons as a function of temperature. The dashed curve shows the free exciton energy from Fig. 3. (c) Donor- and acceptor-bound exciton peak intensities as a function of temperature.

els. The presence of defect-related acceptors in ZnO NCs could also explain the observed PL peak width (~220 meV), because arbitrarily positioned zinc vacancies in ZnO NCs will have different acceptor levels depending on their distance from the NC center. It is seen from Fig. 4 that PL from ZnO NCs is mainly due to recombination of the acceptor-bound excitons for $T<150$ K. For $T>150$ K, the PL is found to be due to recombination of donor-bound excitons. Due to this reason the UV peak observed in the room temperature PL of ZnO NCs (see Fig. 2) has been assigned to recombination of the donor-bound excitons.

Figure 5(a) shows the UV region of PL spectrum of ZnO QDs for temperatures from 8.5 to 150 K. Recalling from the room temperature PL that the main peak in this region is likely due to the acceptor-bound excitons, and using the same order of peaks as in the case of bulk ZnO PL, we can tentatively assign the observed peaks (from right to left) to donor-bound excitons (D, X), acceptor-bound excitons (A, X), and a LO phonon peak of the acceptor-bound excitons. The observed energy of LO phonon is 72 meV (582 cm^{-1}), which is in good agreement with the theoretical and experimental considerations.[6,13,14] An arrow in Fig. 5(a) shows the calculated location of the confined exciton energy (3.462 eV) for ZnO QDs with the diameter of 4.4 nm (the energy corresponding to confined excitons in 4 nm QDs lies outside the range of energies in Fig. 5(a)[5]). Note that at a given laser excitation the larger size QDs from the ensemble of 4 nm±0.8 nm are excited, therefore we attribute the observed PL spectrum to 4.4 nm QDs. No confined exciton peak is seen at 3.462 eV or any other location for all considered temperatures, which might be explained by the presence of the surface acceptor impurities in ZnO QDs. The latter is not surprising given a large surface-to-volume ratio in QDs. It can be estimated from the ZnO lattice constants ($a=0.3249$ nm, $c=0.5207$ nm) that one atom (Zn or O) occupies a volume of a cube with edge $a_0=0.228$ nm. Therefore, one can show that the number of surface atoms in the 4.4 nm ZnO QD constitutes 28% of the total number of atoms in this QD.

Figures 5(b) and 5(c) show the PL peak energies and PL peak intensities of the donor-bound and acceptor-bound excitons extracted from Fig. 5(a). Figure 5(b) and Table I show that the temperature dependence of the energy of the impurity-bound excitons can be described by Varshni law [Eq. (1)], similarly to the case of bulk ZnO. Comparing Figs. 5(b) and 3(b), one can find that the donor-bound exciton energy in 4 nm ZnO QDs is increased by about 5 meV compared to the bulk value due to the quantum confinement of donor-bound excitons. At the same time, a comparison of the acceptor-bound exciton energies in 4 nm ZnO QDs and in bulk ZnO shows a decrease of about 10 meV for ZnO QDs at temperatures up to 70 K. The observed decrease of the energy of the acceptor-bound excitons in ZnO QDs cannot be explained by confinement. One possible explanation could be the lowering of the impurity potential near the QD surface. Another possibility is that at low temperatures this peak is affected by some additional binding similar to that in a charged donor-acceptor pair.[28–30]

The energy of a donor-acceptor pair in bulk ZnO can be calculated as[28]

$$E_{DAP} = E_g - E_D^{\mathrm{bind}} - E_A^{\mathrm{bind}} + \frac{e^2}{4\pi\varepsilon_0\varepsilon R_{DA}}, \qquad (2)$$

where E_g is the band gap (distance between conduction and valence bands), which is 3.437 eV at 2 K, E_D^{bind} is the bind-

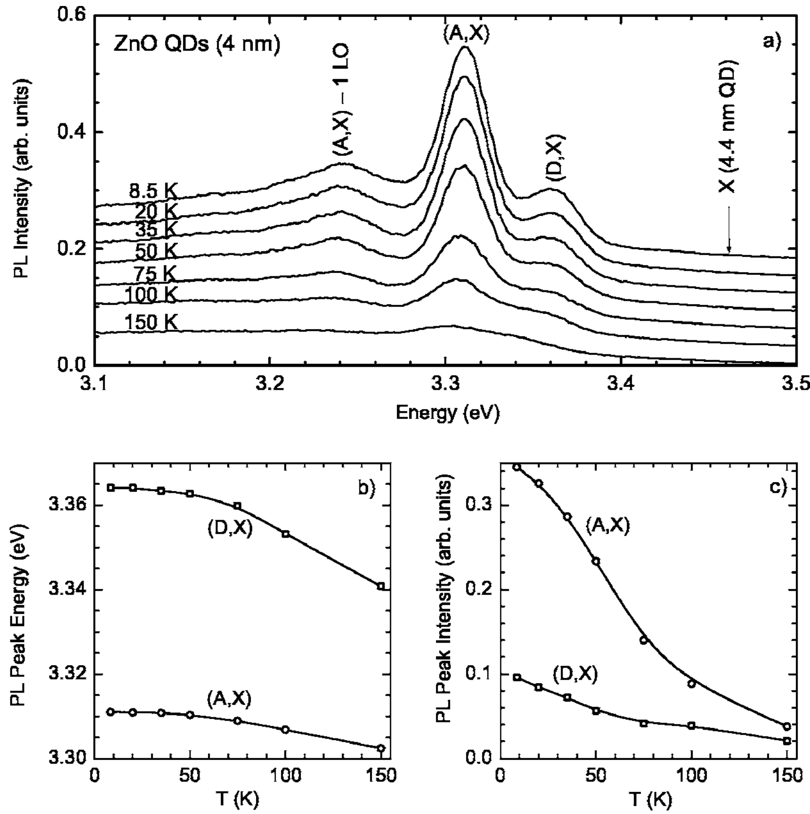

FIG. 5. (a) PL spectra of ZnO quantum dots (4 nm) at temperatures from 8.5 to 150 K. The spectra are shifted in the vertical direction for clarity. The location of the confined exciton peak is marked with an arrow. (b) Peak energies for the donor- and acceptor-bound excitons as a function of temperature. (c) Donor- and acceptor-bound exciton peak intensities as a function of temperature.

ing energy of a donor (energy below the bottom of conduction band), E_A^{bind} is the binding energy of an acceptor (energy above the top of valence band), ε_0 is the permittivity of free space, e is the electron charge, $\varepsilon=8.1$ is the dielectric constant (inverse average of $\varepsilon_\perp=7.8$ and $\varepsilon_\parallel=8.75$), and R_{DA} is the donor-acceptor pair separation. Both electrons and holes are confined inside the ZnO QDs. Therefore, in order to apply Eq. (2) to ZnO QDs, one has to take into account the confinement-induced increase of E_g, E_D^{bind}, and E_A^{bind}. Since E_g and $E_D^{\mathrm{bind}}+E_A^{\mathrm{bind}}$ enter Eq. (2) with opposite signs, the effect of confinement is partially canceled and in the first approximation, one can employ Eq. (2) for ZnO QDs. Note that E_D^{bind} is about 60 meV for ZnO.[28] The large percentage of surface atoms in the 4.4 nm ZnO QD (28%) allows us to assume that the majority of the acceptors are located at the surface, which is also in agreement with our previous theoretical results.[5] Because of a relatively small number of atoms (3748) in the 4.4 nm ZnO QD, it is reasonable to assume that there are only 1–2 donor-acceptor pairs in such QDs. Indeed, a typical concentration of acceptors 10^{19} cm^{-3} [Refs 28,29] means only 0.5 acceptors per volume of our 4.4 nm QD. Thus, the donor-acceptor pair separation R_{DA} is equal to the average distance from the surface acceptor to the randomly located donor. This average distance is exactly equal to the radius of the considered QD. For the observed donor-acceptor pair one can find from Eq. (2): 3311 meV $=3437$ meV-60 meV$-E_A^{\mathrm{bind}}+80.8$ meV. Therefore, the lower limit of the acceptor binding energy is estimated to be $E_A^{\mathrm{bind}}=146.8$ meV, which is in agreement with the reported values 107–212 meV.[17,30] Note that for bulk ZnO, the donor-acceptor peak was observed at 3.216 eV.[34]

IV. ANALYSIS OF THE TEMPERATURE DEPENDENCE OF PL FROM ZnO QDs AND NCs

The PL intensity of the donor-bound excitons and acceptor-bound excitons in ZnO QDs as a function of temperature [see Fig. 5(c)] exhibits a kink at about 70 K. One can also see that the PL intensity of the donor-bound excitons in ZnO NCs manifests a "negative thermal quenching,"[35] i.e., it increases with temperature [see Fig. 4(c)]. To elucidate the origin of these effects we analyzed the integral PL intensity in the UV region. The integral PL intensity usually decreases with temperature due to the thermal quenching as[36]

$$I(T)=\frac{I_0}{1+A\exp\left(-\frac{E_a}{k_BT}\right)}, \tag{3}$$

where I_0 is the peak intensity at temperature $T=0$ K, A is a parameter, E_a is the activation energy in the thermal quenching process, and k_B is the Boltzmann constant. The advantage of having a large exciton binding energy for some device applications is clearly seen from Eq. (3). Indeed, the PL intensity increases almost exponentially with the activation (binding or localization) energy at a given temperature. Figure 6 shows the integral PL intensity calculated in the UV region of energies as a function of the inverse temperature for bulk ZnO, ZnO NCs, and ZnO QDs. The curves in Fig. 6 represent the results of the best fit according to Eq. (3).

In the case of bulk ZnO, the activation energy is found to be 9 meV for $T<70$ K and 59 meV for $T>70$ K. These activation energies reflect very well the properties of PL

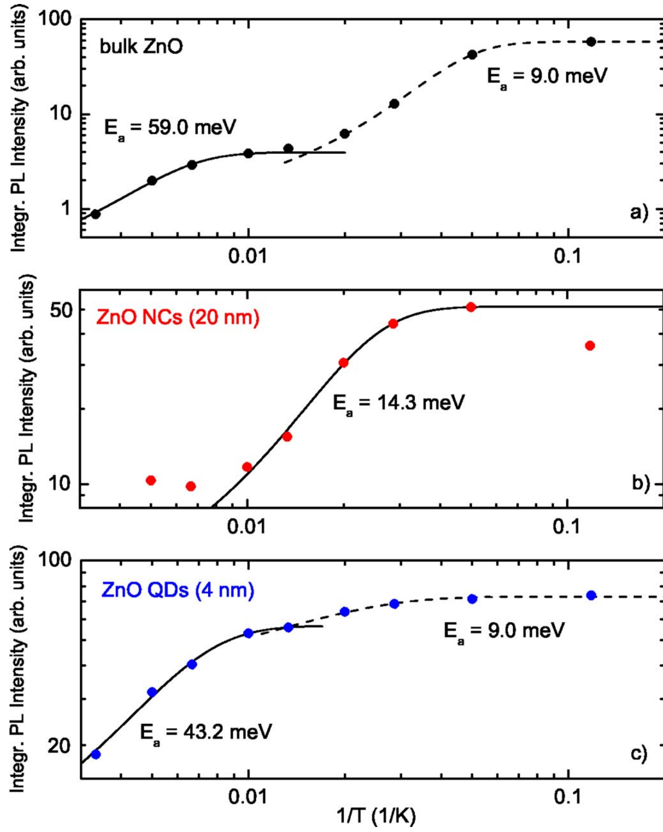

FIG. 6. (Color online). Log-log plot of the integral UV PL intensity as a function of the inverse temperature (from 333 to 5 K) for (a) *a*-plane bulk ZnO, (b) 20 nm ZnO nanocrystals, and (c) 4 nm ZnO quantum dots. Dots represent experimental data, while curves give theoretical fitting. Extracted activation energies of the thermal quenching are shown. The regions of negative thermal quenching seen in the plot (b) are discussed in the text.

spectra in Fig. 3. Namely, for $T<70$ K the PL originates from the recombination of the donor-bound excitons with the localization energy of ~9 meV; while for $T>70$ K the PL originates from the recombination of the free excitons with the binding energy of about ~59 meV. In the case of ZnO NCs [see Fig. 6(b)], the activation energy was found to be 14.3 meV for the temperature range $20\text{ K}<T<100\text{ K}$. Moreover, for the temperatures below 20 K and above 100 K, the negative thermal quenching has been observed. The mechanism of the negative thermal quenching is the thermal activation of carriers with energies smaller than those of the initial state of PL emission.[35] It is possible that for the temperatures below 20 K, there occurs activation of some deep levels, which increases PL intensity with the temperature. At the same time, for the temperatures above 100 K, the activated acceptor levels supply charge carriers for the observed donor-bound exciton recombination at higher energies. The latter can explain the increase of the donor-exciton PL intensity with the temperature observed in Fig. 4.

In the case of ZnO QDs [see Fig. 6(c)], the activation energy is found to be 9 meV for $T<70$ K, while it is 43.2 meV for $T>70$ K. Since the intensity of the donor-bound exciton peak in ZnO QDs is substantially lower than that of the acceptor-bound exciton peak, we assume that the integral PL intensity is due to the acceptor-bound excitons. It is determined that for $T<70$ K the PL peak has the position of the acceptor-bound exciton [see Fig. 5(a)] and the activation energy of 9 meV. The latter suggests that in this temperature region, PL can originate from either the acceptor-bound exciton emission or recombination of the donor-acceptor pairs, where the observed activation energy could be explained by a transition between the acceptor-bound exciton and the donor-acceptor pair energy levels. On the other hand, for $T>70$ K the PL peak has the position of the acceptor-bound exciton and the activation energy of 43.2 meV, which is approximately equal to the difference between donor-bound and acceptor-bound exciton energies. The latter means that in this temperature region, PL is due to the recombination of the acceptor-bound excitons and the activation energy is due to the re-localization (donor-bound $\rightarrow$ acceptor-bound) of the exciton. Correspondingly, the kink observed in Fig. 5(c) is explained by the change in the activation energy at T=70 K. The origin of the observed small values of the low-temperature activation energies in ZnO NCs (14.3 meV) and ZnO QDs (9 meV) could be due to the spatial coupling[37] of ZnO nanostructures in their ensembles.

The temperature dependence (thermal broadening) of the linewidth $\Gamma(T)$, or the full width at half maximum (FWHM), of the free and bound exciton peaks in the PL spectra can be calculated as[38]

$$\Gamma(T)=\Gamma_0+\Gamma_{\mathrm{ph}}\left[\exp\left(\frac{E_{\mathrm{LO}}}{k_BT}\right)-1\right]^{-1}+\Gamma_{\mathrm{imp}}\exp\left(-\frac{E_b}{k_BT}\right), \tag{4}$$

where Γ_0 is the intrinsic linewidth at $T=0$, Γ_{ph} is the exciton-LO phonon coupling constant, E_{LO} is the LO phonon energy, Γ_{imp} is the linewidth due to ionized impurity scattering, and E_b is the average binding energy of the impurity-exciton complexes. As seen from Eq. (4), the temperature dependence of the linewidth allows one to analyze the coupling of excitons to LO phonons, the strength of the ionized impurity scattering, and the average binding energy of the impurity-exciton localization. Figure 7 shows the temperature dependence of the linewidth for the free excitons in bulk ZnO [extracted from Fig. 3(a)] and for the acceptor-bound excitons in ZnO QDs [extracted from Fig. 5(a)]. It is seen from Fig. 7 that the observed linewidths can be fitted perfectly to Eq. (4). The best fit parameters are listed in Table II for free excitons in bulk ZnO and acceptor-bound excitons in ZnO QDs (the LO phonon energy E_{LO} is taken to be 71 meV[13]).

Table II shows that the intrinsic ($T=0$ K) linewidth for ZnO QDs is 3.2 times the intrinsic linewidth of bulk ZnO. This fact can be explained by the additional broadening due to the QD size distribution in the ensemble and the arbitrary impurity positions inside the QD. As seen from Table II, for ZnO QDs the exciton-LO phonon coupling constant is 7.1 times less, while the strength of the ionized impurity scattering is 7.3 times higher than the corresponding values for bulk ZnO. The latter allows us to conclude that the concentration of impurities is higher in ZnO QDs than it is in bulk ZnO.

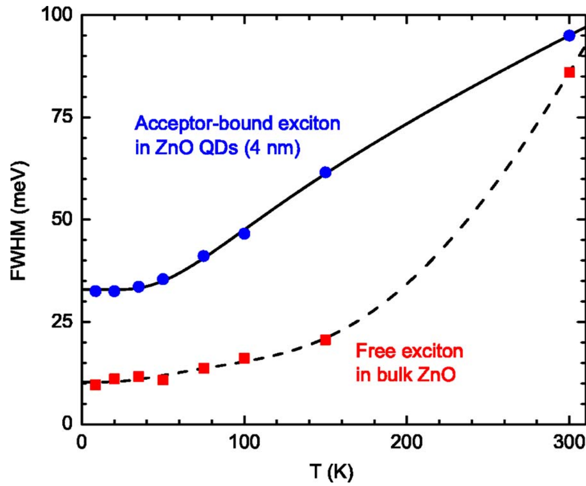

FIG. 7. (Color online). Temperature dependence of the full width at half maximum of the free exciton PL peak in *a* plane bulk ZnO (boxes) and of the acceptor-bound exciton peak in 4 nm ZnO quantum dots (circles). Dashed and solid curves show the best fit to Eq. (4). The full width at half maximum of the acceptor-bound exciton peak in 20 nm ZnO nanocrystals (not shown) is about 220 meV.

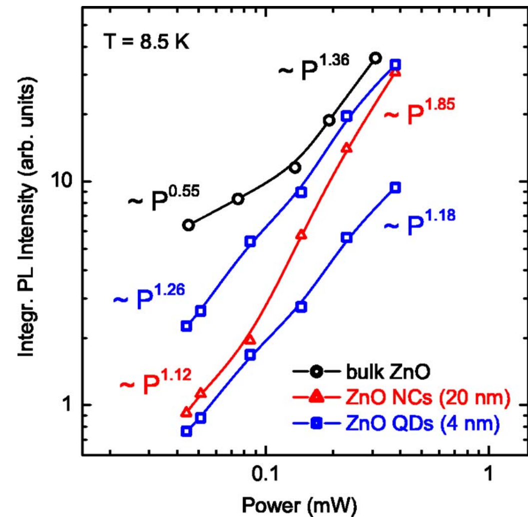

FIG. 8. (Color online). Log-log plot of low-temperature ($T=8.5$ K) integral UV PL from *a*-plane bulk ZnO (circles), 20 nm ZnO nanocrystals (triangles), and 4 nm ZnO quantum dots (squares) as a function of excitation power. For ZnO quantum dots, the power dependence is shown for both acceptor-bound (upper curve) and donor-bound (lower curve) exciton peaks.

Finally, the extracted average binding energy (9.2 meV) of the impurity-exciton complexes that broadens the free exciton emission line in bulk ZnO almost coincides with the donor-exciton localization energy (9 meV) extracted from Fig. 6(a). Therefore, one can say that donors are practically the only impurities in the reference bulk ZnO crystal. On the other hand, the extracted average binding energy (16.6 meV) of the impurity-exciton complexes that broadens the acceptor-bound emission line in ZnO QDs is of the same order of magnitude as the activation energy (9 meV) for the low-temperature acceptor-bound exciton emission in ZnO QDs [see Fig. 6(c)].

In order to verify the mechanisms of the carrier recombination processes determined from the temperature-dependent study (as described above), we have measured the excitation power dependence of the integral UV PL intensity at 8.5 K. Figure 8 shows the obtained power dependence for bulk ZnO (circles), 20 nm ZnO NCs (triangles), and 4 nm ZnO QDs (squares). No significant exciton energy shifts have been observed for different excitation powers. Note that all spectra presented in Figs. 2–5 were taken with the excitation power of ~0.4 mW. It is well established that the PL intensity I increases with the excitation power P as $I \sim P^k$.[39,40] According to the previous studies, which are commonly accepted and independently confirmed for many material systems,[39,40] if the excitation energy is higher than the band gap, which is the case for all our measurements, the power factor k falls into one of the following ranges. It is in the range $1<k<2$ for the bound-exciton emission; and it is in the range $0<k<1$ for the free-to-bound radiative recombination, such as free hole and neutral donor recombination (h, D); free electron and neutral acceptor recombination (e, A); or donor-acceptor pair recombination (D, A). One can see from Fig. 8 that for bulk ZnO, PL intensity increases with excitation power as $P^{0.55}$ for $P<0.1$ mW and as $P^{1.36}$ for $P>0.1$ mW. This means that the observed low-temperature PL is due to (h, D) recombination when $P<0.1$ mW, because concentration of acceptors in bulk ZnO is much less than concentration of donors. When the excitation power increases ($P>0.1$ mW), donor-bound excitons are formed, and their recombination is observed in the PL spectrum.

For ZnO NCs, PL intensity increases with excitation power as $P^{1.12}$ for $P<0.1$ mW and as $P^{1.85}$ for $P>0.1$ mW. This means that the observed low-temperature PL is due to acceptor-bound exciton recombination for all considered excitation powers. The observed superlinear in-

TABLE II. Parameters of the linewidth thermal broadening for the free excitons in bulk ZnO and acceptor-bound excitons in ZnO quantum dots (E_{LO}=71 meV).

	Free exciton in bulk ZnO (*a* plane)	Acceptor-bound exciton in ZnO QDs (4 nm)
Γ_0 (meV)	10.3	32.9
Γ_{ph} (meV)	962.7	136.5
Γ_{imp} (meV)	13.8	100.2
E_b (meV)	9.2	16.6

crease of PL intensity with higher excitation power ($P > 0.1$ mW) could be due to the charge carrier transfer between individual ZnO NCs in the considered ensemble. Finally, for ZnO QDs, Fig. 8 shows the excitation power dependence for both the acceptor-bound (upper curve) and donor-bound (lower curve) exciton peaks. One can see that PL intensity of the donor-bound exciton peak increases with excitation power as $P^{1.18}$ for all considered excitation powers. The latter is in agreement with the assignment made for this peak earlier. At the same time, the intensity of the dominant UV peak in the low-temperature PL of 4 nm ZnO QDs increases with power as $P^{1.26}$ for all considered excitation powers. This fact suggests that the dominant UV peak in ZnO QDs is due to the acceptor-bound exciton recombination rather than due to the donor-acceptor pair recombination.

V. CONCLUSIONS

In conclusion, we have investigated the carrier recombination processes in ZnO QDs and NCs using the PL spectroscopy in the temperature range from 8.5 to 300 K. It has been shown that the ultraviolet PL in 4 nm ZnO QDs originates from recombination of the acceptor-bound excitons for all considered temperatures and excitation powers. At the same time, only the low-temperature ($T < 150$ K) PL from 20 nm ZnO NCs is mainly due to recombination of the acceptor-bound excitons. For higher temperatures ($T > 150$ K), the PL from 20 nm ZnO NCs is due to recombination of the donor-bound excitons. We demonstrated that the recombination processes in ZnO QDs (with the size comparable to the exciton diameter) and in ZnO NCs (with the size much larger than the exciton diameter) differ from those in bulk ZnO mainly because of the large surface-to-volume ratio in both types of nanoparticles and, correspondingly, a high number of acceptor impurities near the surface. The acceptor impurities have been shown to be the main centers of the exciton recombination in ZnO QDs; the acceptors in ZnO NCs are the centers of exciton recombination only at low temperatures ($T < 150$ K); and the acceptors in bulk ZnO are not responsible for the observed exciton recombination. Our experimental findings are in agreement with the theoretical prediction about the role of the surface acceptors in ZnO QDs.[5] The obtained results are important for the proposed optoelectronic and spintronic applications of ZnO nanostructures.

ACKNOWLEDGMENTS

This work has been supported in part by the Microelectronics Advanced Research Corporation (MARCO) and its Focus Center on Functional Engineered Nano Architectonics (FENA) and by the DMEA/DARPA Center for Nanoscience Innovation for Defense (CNID). A.A.B. thanks researchers of the Electronic Device Materials group for their hospitality and useful discussions during his sabbatical at the University of Cambridge, UK.

---

*Electronic address: balandin@ee.ucr.edu; on leave from the Department of Electrical Engineering, University of California—Riverside; present address: Department of Engineering, University of Cambridge, Cambridge, CB2 1PZ, UK.

[1] S. Ghosh, V. Sih, W. H. Lau, D. D. Awschalom, S.-Y. Bae, S. Wang, S. Vaidya, and G. Chapline, Appl. Phys. Lett. **86**, 232507 (2005).

[2] M. Ivill, S. J. Pearton, D. P. Norton, J. Kelly, and A. F. Hebard, J. Appl. Phys. **97**, 053904 (2005).

[3] S. C. Erwin, L. J. Zu, M. I. Haftel, A. L. Efros, T. A. Kennedy, and D. J. Norris, Nature (London) **436**, 91 (2005).

[4] B. K. Meyer, H. Alves, D. M. Hofmann, W. Kriegseis, D. Forster, F. Bertram, J. Christen, A. Hoffmann, M. Strassburg, M. Dworzak, U. Haboeck, and A. V. Rodina, Phys. Status Solidi B **241**, 231 (2004).

[5] V. A. Fonoberov and A. A. Balandin, Appl. Phys. Lett. **85**, 5971 (2004); Phys. Rev. B **70**, 195410 (2004); Appl. Phys. Lett. **86**, 226101 (2005).

[6] V. A. Fonoberov and A. A. Balandin, Phys. Rev. B **70**, 233205 (2004); Phys. Status Solidi C **1**, 2650 (2004); J. Phys.: Condens. Matter **17**, 1085 (2005).

[7] E. M. Wong and P. C. Searson, Appl. Phys. Lett. **74**, 2939 (1999).

[8] S. Mahamuni, K. Borgohain, B. S. Bendre, V. J. Leppert, and S. H. Risbud, J. Appl. Phys. **85**, 2861 (1999).

[9] L. Guo, S. Yang, C. Yang, P. Yu, J. Wang, W. Ge, and G. K. L. Wong, Appl. Phys. Lett. **76**, 2901 (2000).

[10] C. L. Yang, J. N. Wang, W. K. Ge, L. Guo, S. H. Yang, and D. Z. Shen, J. Appl. Phys. **90**, 4489 (2001).

[11] H. Zhou, H. Alves, D. M. Hofmann, W. Kriegseis, B. K. Meyer, G. Kaczmarczyk, and A. Hoffmann, Appl. Phys. Lett. **80**, 210 (2002).

[12] R. D. Yang, S. Tripathy, Y. Li, and H. J. Sue, Chem. Phys. Lett. **411**, 150 (2005).

[13] K. A. Alim, V. A. Fonoberov, and A. A. Balandin, Appl. Phys. Lett. **86**, 053103 (2005).

[14] K. A. Alim, V. A. Fonoberov, M. Shamsa, and A. A. Balandin, J. Appl. Phys. **97**, 124313 (2005).

[15] S. Ozaki, T. Tsuchiya, Y. Inokuchi, and S. Adachi, Phys. Status Solidi A **202**, 1325 (2005).

[16] Y. L. Liu, Y. C. Liu, W. Feng, J. Y. Zhang, Y. M. Lu, D. Z. Shen, X. W. Fan, D. J. Wang, and Q. D. Zhao, J. Chem. Phys. **122**, 174703 (2005).

[17] B. P. Zhang, N. T. Binh, Y. Segawa, K. Wakatsuki, and N. Usami, Appl. Phys. Lett. **83**, 1635 (2003).

[18] H. Najafov, Y. Fukada, S. Ohshio, S. Iida, and H. Saitoh, Jpn. J. Appl. Phys., Part 1 **42**, 3490 (2003).

[19] T. Matsumoto, H. Kato, K. Miyamoto, M. Sano, and E. A. Zhukov, Appl. Phys. Lett. **81**, 1231 (2002).

[20] Y. Zhang, B. Lin, X. Sun, and Z. Fu, Appl. Phys. Lett. **86**, 131910 (2005).

[21] X. T. Zhang, Y. C. Liu, Z. Z. Zhi, J. Y. Zhang, Y. M. Lu, D. Z. Shen, W. Xu, X. W. Fan, and X. G. Kong, J. Lumin. **99**, 149

(2002).
[22] J. Chen and T. Fujita, Jpn. J. Appl. Phys., Part 2 **41**, L203 (2002).
[23] C. R. Gorla, N. W. Emanetoglu, S. Liang, W. E. Mayo, Y. Lu, M. Wraback, and H. Shen, J. Appl. Phys. **85**, 2595 (1999).
[24] D. M. Bagnall, Y. F. Chen, Z. Zhu, T. Yao, M. Y. Shen, and T. Goto, Appl. Phys. Lett. **73**, 1038 (1998).
[25] H. J. Ko, Y. F. Chen, Z. Zhu, T. Yao, I. Kobayashi, and H. Uchiki, Appl. Phys. Lett. **76**, 1905 (2000).
[26] D. G. Kim, T. Terashita, I. Tanaka, and M. Nakayama, Jpn. J. Appl. Phys., Part 2 **42**, L935 (2003).
[27] T. Fujita, J. Chen, and D. Kawaguchi, Jpn. J. Appl. Phys., Part 2 **42**, L834 (2003).
[28] D. C. Look, D. C. Reynolds, C. W. Litton, R. L. Jones, D. B. Eason, and G. Cantwell, Appl. Phys. Lett. **81**, 1830 (2002).
[29] H. W. Liang, Y. M. Lu, D. Z. Shen, Y. C. Liu, J. F. Yan, C. X. Shan, B. H. Li, Z. Z. Zhang, J. Y. Zhang, and X. W. Fan, Phys. Status Solidi A **202**, 1060 (2005).
[30] F. X. Xiu, Z. Yang, L. J. Mandalapu, D. T. Zhao, J. L. Liu, and W. P. Beyermann, Appl. Phys. Lett. **87**, 152101 (2005).
[31] Y. P. Varshni, Physica (Amsterdam) **34**, 149 (1967).
[32] L. Wang and N. C. Giles, J. Appl. Phys. **94**, 973 (2003).
[33] A. R. Hutson, J. Phys. Chem. Solids **8**, 467 (1959).
[34] K. Thonke, T. Gruber, N. Teofilov, R. Schönfelder, A. Waag, and R. Sauer, Physica B **308–310**, 945 (2001).
[35] H. Shibata, Jpn. J. Appl. Phys., Part 1 **37**, 550 (1998).
[36] D. S. Jiang, H. Jung, and K. Ploog, J. Appl. Phys. **64**, 1371 (1988).
[37] A. Nishikawa, Y. G. Hong, and C. W. Tu, J. Vac. Sci. Technol. B **22**, 1515 (2004).
[38] T. Li, H. J. Lozykowski, and J. L. Reno, Phys. Rev. B **46**, 6961 (1992).
[39] T. Schmidt, K. Lischka, and W. Zulehner, Phys. Rev. B **45**, 8989 (1992).
[40] L. Bergman, X.-B. Chen, J. L. Morrison, J. Huso, and A. P. Purdy, J. Appl. Phys. **96**, 675 (2004).